Bulletin of the Seismological Society of America. Vol. 65, No. 1, pp. 55–70. February 1975

PULSE DISTORTION AND HILBERT TRANSFORMATION IN MULTIPLY REFLECTED AND REFRACTED BODY WAVES

BY GEORGE L. CHOY AND PAUL G. RICHARDS

ABSTRACT

Many seismic body waves are associated with rays which are not minimum travel-time paths. Such arrivals contain pulse deformation due to a phase shift in each frequency component. For sufficiently high frequencies, the phase shift each time a ray touches an internal caustic is $\pi/2$ and frequency-independent. The distorting effect of a frequency-independent phase shift is successfully observed in seismograms from events in several regions. The data examined are long-period (T > 9 sec). They include deep earthquakes (depth > 500 km), in which a series of well-separated *S* phases (*S*, *sS*, *SS* and *sSS*) are available. These show that the wave form of *SS*, which has been distorted in propagation through the Earth, can be derived from the wave form of *sS*, which is not distorted. Shallow events, in which multiple *S* phases overlap, also exhibit behavior predicted by phase distortion. Rays supercritically reflected or refracted at a discontinuity in the Earth also suffer a constant phase shift, which in general can have any value. An important case is *SKKS*: its undistorted wave form resembles that of *SKS*, which has a minimum travel-time path.

Without exception, all the distorted wave forms bear little or no resemblance to the original wave form. That is, neither the first arrival of energy nor the subsequent relative position of peaks and troughs on a distorted wave form appear at the ray theoretical times. Thus, *T*-Δ curves constructed by choosing arrival times to correspond to the first arrival of energy may be biased. Similarly, doubt is cast on differential travel times chosen from first motions, or from averaging several points on what appear to be corresponding peaks and troughs of two wave forms. Some of the rays most important to seismology, in which the distortion phenomenon occurs, include *P* and *S* (where $d^2T/d\Delta^2 > 0$), PKP_{AB}, *PP*, *SS*, and *SKKS*. Removal of phase distortion in the data is computationally straightforward. By exploiting the resulting wave forms to full advantage in correctly picking arrival times, we may hope to improve velocity models of the Earth. It is shown that matched filtering to obtain differential travel times is appropriate for certain pairs of body waves if they are phase-corrected.

INTRODUCTION

Wave form distortion may be imposed on a pulse propagating through the Earth by a variety of mechanisms. These include amplitude and phase effects such as attenuation and dispersion. The distortion to be described in this paper occurs in the context of geometrical ray theory, and is present for rays which have touched an internal caustic surface (as in Figure 1). Such rays have the property of a non-minimum travel-time path. Jeffreys and Lapwood (1957) have shown that the deformation incurred at a caustic is, at sufficiently high frequencies, a constant $\pi/2$ phase shift in each frequency component. This type of pulse distortion has been studied in acoustics (Arons and Yennie, 1950; Tolstoy, 1968; Blatstein, 1971; Sachs and Silbiger, 1971). However, it appears the effect has not been explicitly demonstrated in actual seismograms.

It would be important to confirm if the distortion of original pulse shapes is present on seismograms, since the distortion of an impulsive signal will in general develop a precursor. This would invalidate the usual method of making travel-time picks (which is to mark the earliest indication of energy). Furthermore, the distorted body wave bears little, if any, resemblance to the original pulse. Consequently the usual method of calculating differential travel times by picking what appear to be corresponding points (e.g., the peaks or troughs) on two wave forms would be unreliable. This effect is expected to occur in many rays. Some of the more important are *PP*, *SS* and the receding branches of *P*, *S* and *PKP*. Additional phase distortion that is frequency-independent may be introduced by complex transmission and reflection coefficients of a ray which is supercritically reflected or refracted along its path. We shall discuss this for *SKKS*, which also touches an internal caustic, causing an additional $\pi/2$ phase shift.

Rays that Touch a Caustic

Theory

Several theoretical papers have described the existence of pulse distortion for specific rays in simple models. Jeffreys and Lapwood (1957) for a homogeneous fluid sphere and Burridge (1963) for a homogeneous solid sphere, have shown that *pP* and *sS* are minimum

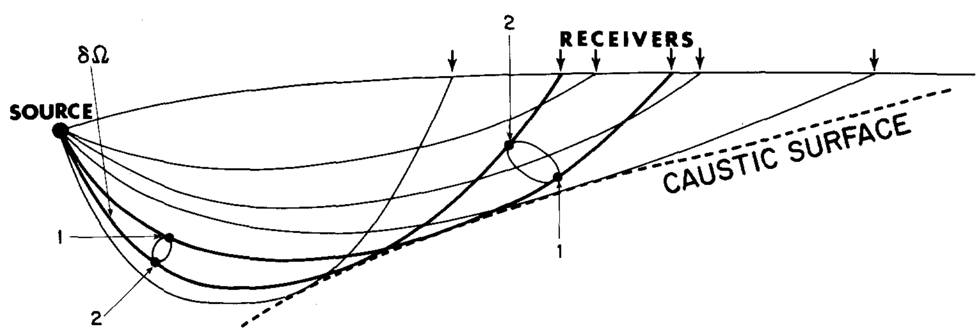

FIG. 1. A point source showing some direct rays and rays returned to the surface after touching a caustic. The caustic surface may be envisioned as the envelope of receding rays. Rays 1 and 2 are each within the surface of a ray tube of cross-sectional area δA. The relative positions of 1 and 2 are reversed at points on opposite sides of the caustic.

time paths and consequently are not phase deformed. *PP* and *SS*, on the other hand, are mini-max travel-time paths for $\Delta < 180°$, and are phase deformed by $\pi/2$ upon touching an internal caustic. Hill (1974), for a point source in a homogeneous fluid half-space overlying a fluid half-space with positive velocity gradient, has shown that higher-order multiple reflections of *P* from below the interface form a series of internal caustics. He predicts which reflections are phase shifted by $\pi/2$. In this and similar fluid models, the phase shift also is in a backward branch of direct *P* (Tolstoy, 1968; Sachs and Silbiger, 1970; and Hill, 1974). We shall show that whenever $d^2T/d\Delta^2 > 0$, the travel time is not a minimum, provided the ray has a turning point.

There are two brief heuristic ways to describe how the phase shift arises in rays which touch a single caustic.

The first way uses geometrical properties of a caustic. Figure 1 sketches a point source and several rays radiating from it which touch an internal caustic surface before returning to the free surface. The ray approximation for a field at a point $\mathbf{x}$ due to a steady-state point source has the form

$$\text{Field }(\mathbf{x}, \omega) = f(\mathbf{x})(\delta\Omega/\delta A)^{1/2} \exp[i\omega(t-\tau)] \tag{1}$$

where δA is the cross-sectional area at $\mathbf{x}$ of the ray tube which departs to $\mathbf{x}$ within some small solid angle $\delta\Omega$ at the source; τ is the travel time along the ray; ω is radian frequency; and $f(\mathbf{x})$ is a real function, which is different for the different physical fields under consideration. The quantity δA has a different sign for two points situated on the same ray and such that the ray touches a caustic between them. Thus, a phase shift of plus or minus $\pi/2$ is introduced by $(\delta A)^{-1/2}$. Since there is a requirement that the synthesized field in the time domain be real,

$$\text{Field}\ (\mathbf{x}, -\omega) = [\text{Field}\ (\mathbf{x}, +\omega)]^*$$

(where $[F]^*$ denotes the complex conjugate of F). Thus, the phase shift has a different sign for positive and negative frequencies. That is, the phase jump is either $\operatorname{sgn}(\omega)\,\pi/2$, or $-\operatorname{sgn}(\omega)\,\pi/2$, (where $\operatorname{sgn}(\omega) = \pm 1$ according as $\omega \gtrless 0$). The final choice of sign here depends on the convention of our Fourier transform.

A second way of viewing the phase shift is to consider how one might evaluate the displacement due to, say, a point source, by the method of steepest descent. Multipath arrivals, involving different ray parameters for the arrivals corresponding to separate branches on a $T-\Delta$ curve, can each be evaluated by an integral in the complex ray para-

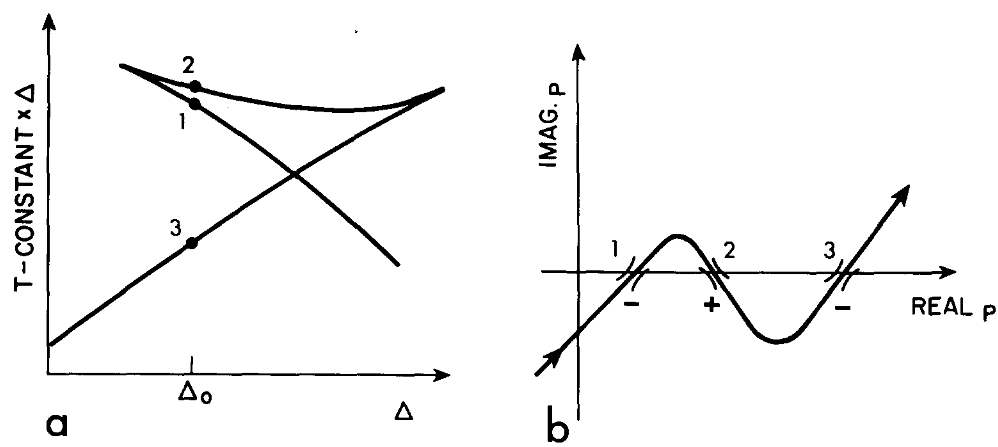

FIG. 2. (*a*) A reduced $T-\Delta$ curve showing a triplication. At Δ_o, there are three arrivals. The first and third fall on forward branches and the second on a receding branch. (*b*) Integration path in the complex ray parameter plane crossing three saddles, each at a value of p (ray parameter) satisfying $\Delta(p) = \Delta_o$. The $(-)$ and $(+)$ signs indicate the sign of $d^2T/d\Delta^2$ at each saddle point. (Modified from Richards, 1973).

meter plane (see Richards, 1973, equation 13). To see that there is a phase shift in arrivals corresponding to the backward branch, we note that the displacement integral for a specific distance, Δ_o, has the phase factor $\exp[i\omega J(p)]$, where

$$J(p) = T(p) - p\Delta(p) + p\Delta_o \tag{2}$$

$T(p)$ and $\Delta(p)$ are the time and distance functions for the Earth, and a ray arriving at the distance of interest (Δ_o) must have a ray parameter p_o such that $\Delta(p_o) = \Delta_o$. For high frequencies, the body-wave displacement can be approximated by the standard asymptotic method of integrating over a saddle point. By solving for p in $\partial J/\partial p = 0$, one finds saddle points occurring at values of p such that $\Delta(p) = \Delta_o$, i.e., at just the ray parameters for which there is a ray between source and receiver. Near such a saddle point, p_o, $J(p)$ may be approximated (using a Taylor series, and $d\Delta/dp = 1/(d^2T/d\Delta^2)$) by

$$J(p) = T(p_o) - \tfrac{1}{2}(p-p_o)^2(d^2T/d\Delta^2)^{-1} \tag{3}$$

In this form, it becomes clear that the sign of $d^2T/d\Delta^2$ will influence the orientation (in the complex ray parameter plane) of the path of steepest descent. Such a path has near p_o the property that

$$\exp(i\omega J) = \exp(i\omega T_o)\exp(-A^2) \tag{4}$$

where A is real and positive. It follows from (3) and (4) that

$$p-p_o = A[(-2i/\omega)(d^2T/d\Delta^2)]^{1/2} \tag{5}$$

so the path of integration makes an angle $\pm\pi/4$ to the real p axis, according as $d^2T/d\Delta^2$ is $\lessgtr 0$. Figure 2a shows a $T-\Delta$ curve with a triplication, and Figure 2b gives the integration path. For each successive arrival, $d^2T/d\Delta^2$ is alternately negative and positive: the steepest descent contribution from each saddle then has a frequency-independent factor of either $\exp(i\pi/4)$ or $\exp(-i\pi/4)$, giving rise to the $\pi/2$ phase shift we seek to explain. (The phase shift we have just found is $-\pi/2$ for the positive frequencies in the non-minimum time arrival, with respect to the minimum time arrival. This discussion was based on full wave theory which conventionally uses $F(\omega) = \int_{-\infty}^{\infty} f(t)\exp(i\omega t)\,dt$ for the Fourier transform of $f(t)$. In the following we shall use the other, more common, sign convention for the Fourier transform, so the associated phase shift used below is $+\pi/2$.)

We note that whenever $d^2T/d\Delta^2 > 0$ and the ray has a turning point, the ray path has a "maximum time" property for perturbations in the vertical plane containing source and receiver. To see this, consider a slight perturbation in which the ray parameter p become $p+\delta p$, so that the perturbed ray passes through a point somewhat displaced radially from the original turning point. The corresponding perturbation in travel time is given by Richards (1971, p. 466) as

$$\delta T = -1/2(\delta p)^2(d^2T/d\Delta^2)^{-1} \tag{6}$$

where δp = ray parameter increment. A travel-time for this particular perturbation is thus minimum (maximum) if δT is positive (negative), but the sign of δT is opposite that of $d^2T/d\Delta^2$.

Although the analysis of Figure 1 is directly applicable to SS (for it touches an internal caustic), the configuration of saddle points in Figure 2 does not apply to the relationship of sS and SS, since both these arrivals have $d^2T/d\Delta^2 < 0$. However, SS has one more turning point than sS, which introduces an extra $\pi/2$ phase shift in the integrand for which a saddle point analysis is carried out.

In the time domain, several equivalent methods can be used to find the effect of a $\mathrm{sgn}(\omega)\pi/2$ phase shift in each frequency component. For the signal $f(t)$, with Fourier transform $F(\omega) = \int_{-\infty}^{\infty} f(t)\exp(-i\omega t)\,dt$, the phase-distorted signal in the time domain is

$$\frac{1}{2\pi}\int_{-\infty}^{\infty}\exp\left(\frac{+i\pi}{2}\,\mathrm{sgn}(\omega)\right)F(\omega)\exp(i\omega t)\,d\omega \tag{7}$$

Substituting for $F(\omega)$ in (7), we obtain the equivalent formula

$$\frac{1}{\pi}\int_{0}^{\infty}d\omega\int_{-\infty}^{\infty}f(\tau)\sin\omega(\tau-t)\,d\tau, \tag{8}$$

which Titchmarsh (1926) and Jeffreys and Jeffreys (1956) have called the allied function of $f(t)$. Integrating over ω in (8), one finds also the form

$$\frac{1}{\pi}\int_{-\infty}^{\infty}\frac{f(\tau)}{\tau-t}\,d\tau \tag{9}$$

in which the singularity at $\tau = t$ is handled by taking the principal value of the integral, i.e., by canceling the singular contributions from τ just greater and just less than t.

The form (9) is one definition of the Hilbert transform of $f(t)$, which we symbolize by $H[f(t)]$. It can also be seen as a convolution (denoted by *) so the final equivalent form for the distorted signal is

$$f(t) * (-1/\pi t). \tag{10}$$

We shall loosely refer to any one of the versions (7), (8), (9), (10) as the Hilbert transform of $f(t)$. In practice, when this transform is to be computed, the original form (7) is most straightforward: one fast Fourier transform gives $F(\omega)$, and the $\pi/2$ phase shift reduces to an interchange of real and imaginary parts of $F(\omega)$ (with a sign change in the resulting real part). An inverse finite Fourier transform then returns the required $H[f(t)]$.

If the Hilbert transform pair, $f(t)$ and $H[f(t)]$, are themselves Hilbert transformed, the resulting pair is $H[f(t)]$ and $-f(t)$. The polarity reversal is simply a result of two $\pi/2$ phase shifts.

The instrument response is not needed in the computation to remove distortion. This follows because the signal on a seismogram is, say, $s_1(t) = f(t)*g(t)$, for incident wave form $f(t)$, where $g(t)$ is the unit pulse response of the instrument. When the incident wave

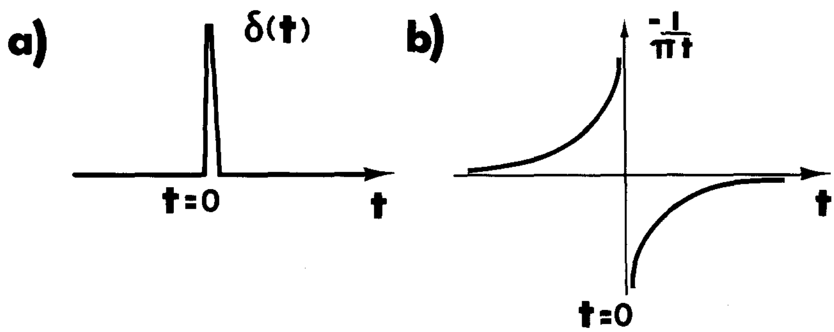

FIG. 3. (*a*) A delta function arriving at a time $t = 0$. (*b*) The Hilbert transform of $\delta(t)$, $(-1/\pi t)$. Note that energy arrives before the ray arrival time.

form is the Hilbert transform, $H[f(t)]$, then the seismic record shows $s_2(t) = H[f(t)]*g(t)$. Viewing the Hilbert transform as a convolution, it is easy to see that $H[s_1(t)] = s_2(t)$.

In general, the wave form of $f(t)$ bears no resemblance to $H[f(t)]$. The Hilbert transform makes all impulsive functions emergent and makes some emergent functions impulsive. A drastic example is the distortion of a unit spike, $\delta(t)$. Figure 3 shows the distortion in this case, and Hilbert transformation obviously obscures the true arrival time.

Observations

(*a*) *Deep earthquakes.* The events used here are all deeper than 500 km, and therefore provide a group of well-separated body waves: *S*, *sS*, *SS* and *sSS*. All data in this paper use records obtained from long-period WWSSN or high-gain long-period (HGLP) stations (Savino *et al.*, 1972) or long-period seismograms from the PAL station.

The once reflected waves, *sS* and *SS*, differ in that *sS* does not touch a caustic but *SS* does. To establish their Hilbert transform relationships, we introduce a symbolic notation for *sS* and *SS*. The body wave *sS* is derived from an *S* wave by convolution with a transfer function T_1

$$sS = S^*T_1$$

T_1 accounts for frequency-dependent crustal and mantle transfer functions along the ray and upon the reflection and all effects except that due to touching a caustic. Similarly, SS is derived from an S wave by convolution with another transfer function, T_2, but it is also Hilbert transformed by touching a caustic, so

$$SS = H(S^*T_2)$$

If the data are long-period and recorded at teleseismic distances, the transfer functions involve only gross features of the mantle and crust. Thus, T_1 and T_2 are expected to be nearly identical except for a multiplicative scalar. The scalar accounts for any amplitude disparity between sS and SS caused by geometrical spreading along different paths. The effect of radiation pattern also reduces to a scalar provided the takeoff angles of sS and SS with respect to the slip direction of the fault plane are nearly the same. We emphasize, therefore, that in our data it is wave form shape, and not amplitude, that we are concerned with. For convenience, T will be used wherever T_1 and T_2 are identical except for a constant.

If a Hilbert transform is applied to sS, a wave form resembling SS should result,

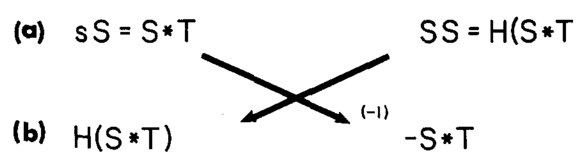

FIG. 4. (*a*) Symbolic representation of a seismogram containing sS and SS. T is the transfer function which accounts for all the frequency-dependent effects along the ray path except the effect of touching a caustic. (*b*) Seismogram after Hilbert transformation. Cross arrows point to equalities in wave form shape, not amplitude.

$$H(sS) = H(S^*T) = SS$$

A second Hilbert transform merely gives the opposite sign. So the Hilbert transform of SS should resemble sS with reversed polarity,

$$H(SS) = H(H(S^*T)) = -S^*T = -sS$$

The relations are summarized in Figure 4. Figure 4a represents a seismogram with sS and SS. Figure 4b represents the seismogram after the whole record is Hilbert transformed. Cross arrows point to the wave shape equalities to expect for the data in Figures 5 to 7. The notation (-1) denotes an equality after polarity reversal of that particular seismogram section.

If, on the focal sphere, sS and SS emerge with opposite polarities, the expected relationships displayed in Figure 4 require modification. For the cross arrow similarities to hold, it is sufficient to reverse polarity for the lower (Hilbert transformed) record.

Confirmation of pulse distortion in real data is found for deep earthquakes. Examples from three different regions are shown in Figures 5 to 7. Only the transverse components are shown, since this allows us to study SH motion uncontaminated by SV, PL-coupled or mode-converted energy. The upper record in each figure is the original seismogram. This time series was Hilbert transformed, and is shown as the lower record in each Figure, after any necessary polarity correction for focal mechanism. In every case, sS does not resemble SS. However, the wave shapes related by the cross arrows verify that sS and SS are a Hilbert transform pair: the wave form of either one can be derived from the Hilbert transform of the other.

(*b*) *Shallow earthquakes.* The Hilbert transformation is also exhibited for shallow earthquakes (< 30 km depth). In these cases, "S" and "SS" are actually S plus sS, and SS

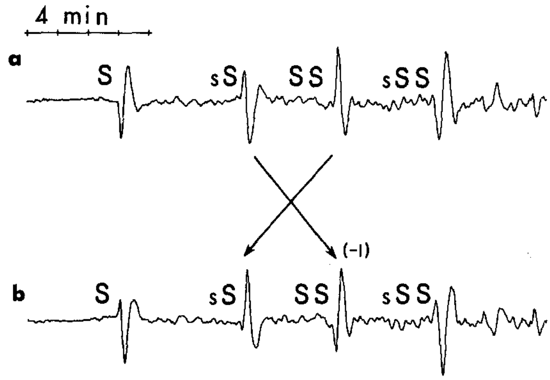

FIG. 5. (*a*) Original EW (transverse) seismogram. Sea of Japan October 8, 1960, OT 05h 53m 01.1s; 40.0N, 129.7E, depth 608 km, m_b 6.5. Recorded at PAL, $\Delta = 96.3°$. (*b*) The Hilbert transform of (*a*). For convenience $H(S)$ is still labeled *S*, and similarly for *sS*, *SS* and *sSS*. The arrows indicate which pair of wave shapes are identical (the notation (-1) indicates a polarity reversal is required to see the similarity). A polarity reversal for focal mechanism correction was applied.

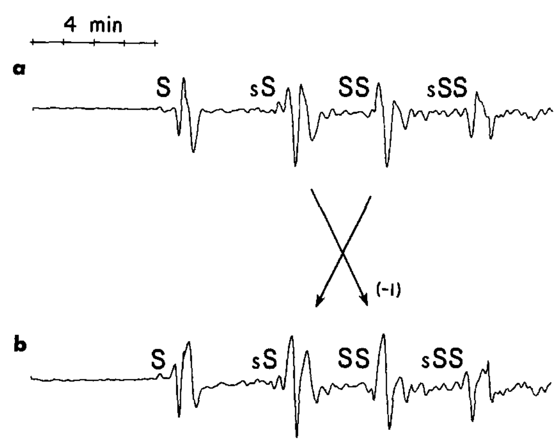

FIG. 6. (*a*) Original EW (transverse) seismogram. Northeast USSR, September 10, 1973, OT 07h 43m 30.5s, 42.5N 130.9E, depth 532 km, m_b 6.0. Recorded at OGD (HGLP), $\Delta = 97.3°$. (*b*) The Hilbert transform of (*a*). A polarity reversal for focal mechanism was applied.

FIG. 7. (*a*) Original NS (transverse) seismogram. Fiji, January 26, 1972, OT 23h 00m 24.2s, 20.2S, 178.0E, m_b 5.7, M_S 6.3, depth 668 km. Recorded at OGD (HGLP), $\Delta = 116.0°$. (*b*) The Hilbert transform of (*a*). Due to radiation pattern the relative amplitude of *SS* is much greater than *sS*. Compare the shapes and not relative amplitudes. A polarity reversal for focal mechanism was applied.

plus *sSS*. If the amplitude ratio of *S* to *sS* is nearly identical to the ratio of *SS* to *sSS*, then, by the linearity property of the Hilbert transform, the body wave formed by the sum of $S+sS$ and the body wave formed by the sum of $SS+sSS$ are also Hilbert trans-

(a) $S + sS = S + S*T$ $\quad$ $SS + sSS = H(S*T)+H(S*T*T)$

(b) $H(S)+H(S*T)$ $\quad$ (-1) $-(S*T)-(S*T*T)$

FIG. 8. (*a*) Symbolic notation of seismogram for shallow earthquake. (*b*) Hilbert transform of above. Cross arrows point to equalities in wave form shape, not amplitude equalities.

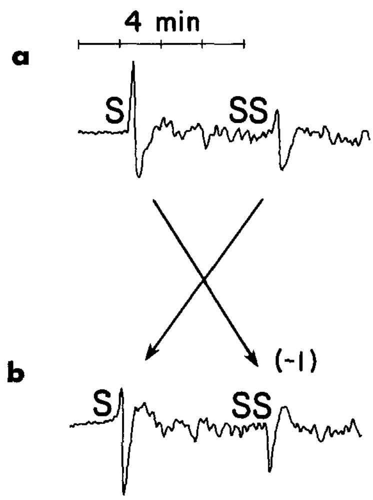

FIG. 9. (*a*) Original EW (transverse) seismogram. East Pacific Rise, March 7, 1963, OT 05h 22m 01.1s, 27.0S, 113.5W, depth < 30 km, m_b 5.6, M_S 6.75. Recorded at TUC, Δ = 59.0°. This has a strike-slip focal mechanism. *S* is actually $S+sS$ and *SS* is actually $SS+sSS$. (*b*) The Hilbert transform of (*a*). For convenience, we still use label *S* and *SS* instead $H(S)$ and $H(SS)$.

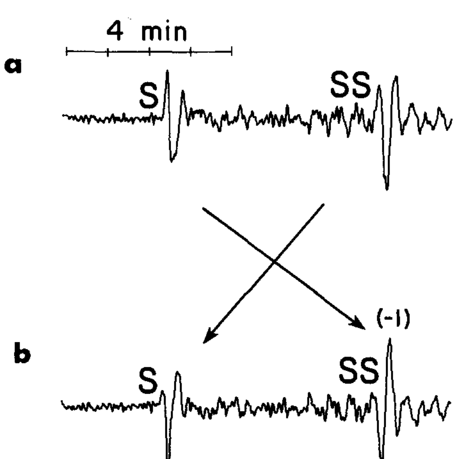

FIG. 10. (*a*) Original EW (transverse) seismogram. South Pacific Ocean, May 9, 1971, OT 08h 25m 01.7s, 39.8S, 104.8W, depth < 30 km, m_b 6.2, M_s 6.0. Recorded at DUG, 80.0°. This has a thrust mechanism. (*b*) The Hilbert transform of (*a*).

form pairs. The top of Figure 8 represents such a seismogram and its Hilbert transform is the lower part of the figure. The wave shape equalities we expect are indicated by the cross arrows. For the cross arrow relationships to hold, two convolutions with *T* must reduce to scalar multiplication by a constant. This would be the case, if *T* were due simply to the *SH* reflection from a free surface. Figures 9 and 10 do show the Hilbert transform relations. The transverse components of the original seismograms are shown at the *top*, and Hilbert transformed seismograms at the *bottom*. The phase shift is not a source effect. Thus, it is observed even though the events have different focal mechanisms: strike-slip for the East Pacific Rise event and intraplate thrust for the South Pacific Ocean event.

We emphasize that in none of the events studied were there any failures: the Hilbert transformation was always observed as long as the transverse component was used. Except in isolated instances, the radial and vertical components did not show the Hilbert transformation property for reflected *SV* or *PP*. Apparently, mode-converted and *PL* energy severely contaminated the phase spectra of these body waves. Polarization filters (e.g., see Choy and McCamy, 1972) applied to these components can help by suppressing energy with other than body-wave polarization. Nevertheless, it is clear from Figures 5 to 10 that phase distortion does occur for rays touching a caustic. Thus, it is still appropriate and necessary to remove the $\pi/2$ phase distortion, even if not readily seen, prior to using arrivals like *PP* or *SS* for travel-time or normal mode purposes. This is equally true for *P*, *S* and *PKP* where $d^2T/d\Delta^2 > 0$.

Supercritically Reflected and Refracted Waves

Theory

Arons and Yennie (1950) have pointed out that if an incoming wave $f(t)$ suffers a phase shift ε, with reflection or refraction coefficient R, then the outgoing wave $f^R(t)$ may be calculated from a linear combination of $f(t)$ and its Hilbert transform. The large class of seismological examples of such phase shifts includes all rays which are supercritically reflected or refracted at a discontinuity such as the Earth's free surface, ocean bottom, crust or core-mantle boundary. Constants in the linear relation are dependent on the phase shift and may be derived as follows

$$\begin{aligned} f^R(t) &= (1/2\pi) \int_{-\infty}^{\infty} R \exp[i \operatorname{sgn}(\omega)\varepsilon] F(\omega) \exp(i\omega t)\, d\omega \\ &= (1/2\pi) \int_{-\infty}^{\infty} R[\cos \varepsilon + i \operatorname{sgn}(\omega) \sin \varepsilon] F(\omega) \exp(i\omega t)\, d\omega \\ &= R\{\cos \varepsilon\, f(t) + \sin \varepsilon\, H[f(t)]\}. \end{aligned} \tag{11}$$

Seeking to retrieve the original pulse shape, we go one step further and take the Hilbert transform of (11),

$$H[f^R(t)] = R\{-\sin \varepsilon\, f(t) + \cos \varepsilon\, H[f(t)]\}. \tag{12}$$

From (11) and (12) it follows that the original pulse $f(t)$ is found in terms of the recorded signal and its Hilbert transform,

$$f(t) = (1/R)\{\cos \varepsilon\, f^R(t) - \sin \varepsilon\, H[f^R(t)]\} \tag{13}$$

(this is equivalent to reversing the role of f and f^R in (11), and phase shifting by $-\varepsilon$).

Data Analysis

To simulate the effect of different phase shifts on an undistorted wave form, we phase shifted an original *S* wave in 10° increments between 0° and 90° (Figure 11) by using equation (11). Typically, for long-period data, a fairly wide range of phase shifts (say, $\pm 15°$) still results in a small time shift (about 1.5 sec).

An important example of a phase shift other than $\pi/2$ occurs in the core phase *SKKS*. A phase shift is introduced for each of the three interactions of *SKKS* with the core-mantle boundary, provided the ray parameter would make the turning point for *P* waves

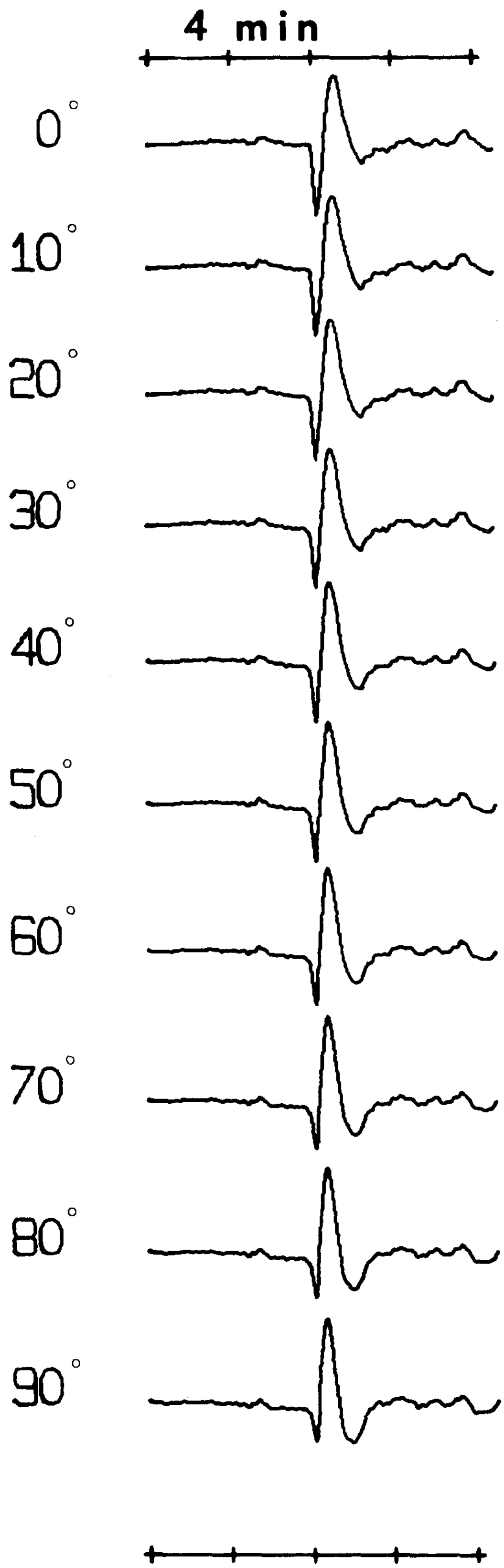

FIG. 11. An S wave is subjected to phase shift in 10° increments, starting with the original signal (0° and ending with the Hilbert transform (90°). The S wave is from the event in Figure 6.

in the mantle. The resulting inhomogeneous P waves decay with depth and a phase shift arises from the reflection-transmission coefficients at the core-mantle boundary. This deformation is in addition to the $\pi/2$ phase shift incurred at a caustic. Thus, *SKKS* recorded on a seismogram has the form $H[f^R(t)]$. Phase distortion of *SKKS* can be

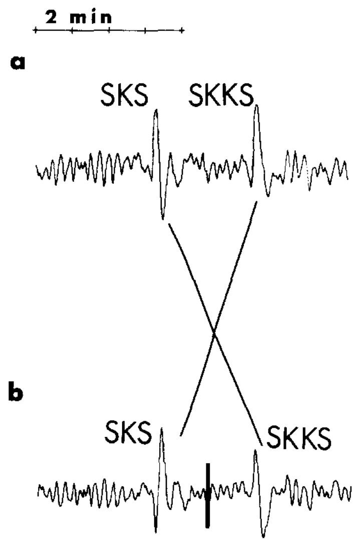

FIG. 12. (*a*) An *SKS-SKKS* pair. Original EW (radial) seismogram. Fiji, November 20, 1971, OT 07h 28m 01.1s, 23.4S, 179.9W, depth 551 km, m_b 6.0. Recorded at OGD (WWSSN), $\Delta = 116.0°$. (*b*) A composite seismogram in which *SKS* and *SKKS*, separated by a vertical line, are processed with different windows. The *SKS* here, having been phase shifted the same amount *SKKS* was shifted in the Earth, now resembles *SKKS*. Conversely, *SKKS*, after removing distortion, now resembles the original *SKS*. Time base relative to the original record is preserved.

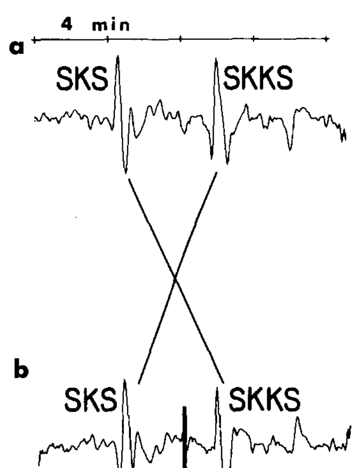

FIG. 13. (*a*) An *SKS-SKKS* pair. Original EW (radial) seismogram. Fiji, July 21, 1973, OT 04h 19m 17.1s, 24.8S, 179.2W, 411 km, m_b 5.9. Recorded at OGD (WWSSN), $\Delta = 116.5°$. (*b*) Composite seismogram. See Figure 12b for explanation.

removed by applying equation (13). Since *SKS* is a minimum travel-time ray, and its ray parameter is small enough not to incur phase shifts in crossing the core-mantle boundary, its wave form is a reasonable approximation to what $f(t)$, the undistorted wave form, would look like. Furthermore, knowing the phase shift, *SKS* can be phase-shifted to look like *SKKS* using equation (11). Three events showing *SKS-SKKS* pairs are shown in

Figures 12 to 14. The *top trace* in each figure is the radial component of the original seismogram. The *bottom trace* is a composite seismogram in which two windows, containing *SKS* and *SKKS*, are treated with different operations. *SKKS*, after being corrected for the phase deformation introduced at the caustic and at each core-mantle interaction, now looks like *SKS*. Conversely, after being phase-shifted by the same angle but with the opposite orientation, *SKS* now resembles *SKKS* of the original seismogram.

CONSEQUENCES OF PULSE DEFORMATION IN SEISMOGRAMS

The analysis of pulse distortion predicts that a sufficiently impulsive function will develop a precursor upon Hilbert transformation. In having verified the existence of pulse distortion in data, we must question the present methodology of constructing travel-time curves. T-Δ curves for non-minimum travel-time rays like *SKKS* may actually be based on times picked earlier than the true ray theoretical time. To test for bias, absolute

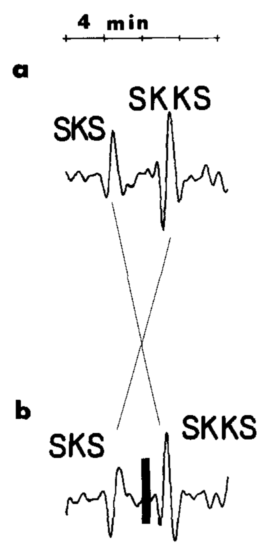

FIG. 14. (*a*) An *SKS*-*SKKS* pair. Original EW (radial) seismogram. South Kermadec, August 22 1973, OT 06h 39m 21.4s, 32.8S, 179.2W, m_b 5.5, M_S 6.0, depth $<$ 30 km. Recorded at OGD (HGLP), Δ = 122.0°. (*b*) Composite seismogram. See Figure 12b for explanation.

and differential travel times for *SS* and *SKKS* were compared before and after these waves were corrected for phase shift. We examined several long-period records, including the examples shown so far.

The data we used for absolute travel time fall into two classes. The first is where the phase-corrected wave form of a seismically recorded signal has an unambiguous nearly impulsive first motion (see *SS* in Figures 9 and 10; and *SKKS* in Figures 12 and 13). A preliminary result is that the arrival times of these phase-corrected wave forms are found to be systematically later with respect to the originally recorded form by up to about four or more seconds. The second class of data is the case where both the recorded and phase-corrected signals have an emergent or ambiguous first motion (see *SS* in Figures 6 and 7), which could be due to a wave form which is inherently emergent or to high noise level, including unwanted seismic energy like codas of body waves. For this type of data, the travel times picked before and after phase-correction usually did not differ significantly. This is not surprising, for in signals with a narrow frequency band such as long-period data, the effect of pulse distortion is manifested more conspicuously as a constant shift of the peaks and troughs of a wave form than as an emergent onset.

Differential travel times between two body waves are commonly used in studies of the Earth's interior. We now examine the error where, because one of the body waves is too emergent to choose a time of first arrival, the differential travel time is taken as the interval between the first prominent features (peaks and troughs) of the two body waves. The intervals between several peaks and troughs may be averaged if the two wave forms appear very similar. We have already pointed out, however, that the positions of peaks and troughs are even more subject to phase shifts than the first arrivals. For example, the relative positions of the first peak of *SKKS* in *a* and *b* in Figures 12 and 13 differ by about 4 sec. Two sources of scatter in differential travel times are possible. First, as discussed previously, a systematic bias can be introduced if the phase shift of a peak (or trough) is not corrected. Second, there is no simple relation governing the behavior of peaks and troughs of any individual body wave before and after distortion: so, in using an original but distorted wave form, it is not predictable whether a record reader would pick a peak

FIG. 15. (*a*) Composite seismogram with *sS* and *H*(*SS*). This event is from the Sea of Japan (see Figure 6). Left of the vertical line, *S* and *sS* come from Figure 6a. Right of the vertical line, *H*(*SS*) and *H*(*sSS*) come from Figure 6b with a polarity reversal. Time base relative to the original record is preserved. (*b*) *sS* from the Sea of Japan event. It is used as the match filter for the composite seismogram. (*c*) The autocorrelation of *sS*. (*d*) Seismogram in (*a*) after match filtering with *sS*. The two central peaks look like the autocorrelation function of the match filter and correspond to the times of best correlation of *sS* with itself and with *H*(*SS*).

later or earlier with respect to the position of the phase-corrected peak. This would result in non-systematic errors. We used our data to obtain peak-to-peak differential travel times: one set of values chosen before and one set chosen after phase-correction. We found that the two sets of values did not differ systematically, suggesting that the second error was dominant.

As a further test, we read differential times from first motions of body waves which were sufficiently impulsive after phase-correction, and compared this new set of times with the peak-to-peak differential times. Indeed, the peak-to-peak times obtained from corrected wave forms agreed much better with this new set of values by several seconds than those values obtained from uncorrected wave forms. It appears that the scatter of differential times will be reduced if waves which have been phase-shifted in propagation through the Earth are corrected prior to use.

The similarity in wave form after phase correction makes matched filtering an appropriate tool to obtain differential travel times for body waves which are Hilbert transform pairs. The process involves cross-correlating one signal, the filter, with another signal. The composite seismograms of Figures 15a and 16a, for instance, show that *sS* and *SKS* because of their similarity in wave form to *H*(*SS*) and phase-corrected *SKKS*, respectively, would be ideal matched filters to obtain true *sS*-*SS* and *SKS*-*SKKS* differential travel times. The filters chosen for our examples (Figures 15b and 16b) are first matched with themselves to obtain their autocorrelation functions (Figures 15c and 16c). They are next cross-correlated with the composite seismograms to give Figures 15d and 16d. The peaks which resemble the autocorrelation functions indicate the time of best correlation between *sS*, *H*(*SS*), *SKS* and phase-corrected *SKKS* with their respective matched filters. The differential travel time is the interval between the appropriate peaks.

This technique has two advantages. First, the times of best correlation obtained from matched filtering effectively average differential times over the entire wave form of each

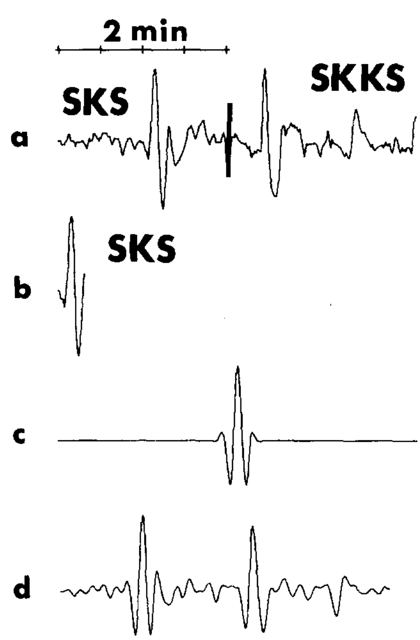

FIG. 16. (*a*) Composite seismogram with *SKS* and phase corrected *SKKS*. This event is from Fiji (see Figure 14). Left of the vertical line, *SKS* comes from Figure 14a. Right of the line, phase corrected *SKKS* comes from Figure 14b. The time base is preserved. (*b*) *SKS* from the Fiji event. It is used as the match filter for the composite seismogram. (*c*) The autocorrelation of *SKS*. (*d*) Seismogram in (*a*) after match filtering with *SKS*. The two peaks look like the autocorrelation function of the match filter and correspond to the times of best correlation of *SKS* with itself and with phase-corrected *SKKS*.

body wave. Second, the window of the wave form used as a match filter is not critical. As long as the principal part of the wave form is recognizable and is included in the filter, the output will have peaks resembling the autocorrelation function at the arrival time of the matching signals. This is a particularly valuable feature where the first arrival of energy is ambiguous.

The wave form of Hilbert transform pairs may also be exploited in studies of multi-branched travel-time curves. A major problem here is in deciding to which branch (receding or forward) a particular arrival belongs. By first deciding whether the arrival has the $\pi/2$ phase distortion, one finds justification for placing it on a forward ($d^2T/d\Delta^2 < 0$) or receding ($d^2T/d\Delta^2 > 0$) branch of the travel-time curve. Note this procedure is valid in the general case of cusps, as well as caustics.

Amplitude attenuation studies are not affected by the phase deformation we are describing in this paper, since any frequency which is phase shifted due to an attenuation process will still be phase shifted $\pi/2$ when a ray touches a caustic. The data have shown that a single Hilbert transform, along with a correction for any phase shift due to supercritical reflection or refraction, is sufficient to invert the phase shift introduced upon touching a caustic.

Conclusions

We have demonstrated that phase distortion is observable in real seismic data. This has been explicitly shown for several events from different regions at different depths with different focal mechanisms. Pulse distortion may be removed with Hilbert transform techniques, whether the phase shift was incurred by touching a caustic and/or by supercritical reflection or refraction.

We have suggested ways to exploit phase-corrected wave forms to fuller advantage. In particular, differential travel times can be improved by removal of phase distortion in the wave forms, and by matched filtering of phase-corrected wave forms.

One must be extremely wary of pulse distortion when choosing travel times. The observations strongly suggest that existing travel-time data be re-examined for possible systematic biases. Bias must be suspected for the receding branches of *P*, *S* and *PKP*, as well as the body waves *SKKS*, *PP* and *SS*.

Acknowledgment

We thank Dr. K. McCamy for valuable discussions; Drs. K. H. Jacob, D. Simpson, and L. R. Sykes for critically reviewing this manuscript; Dr. D. P. Hill for catching an error of substance in an early draft; and Dr. D. Forsyth for aid in finding some examples of the distortion phenomenon. This research was supported by Grant GA 34109 from the Earth Sciences Section, National Science Foundation. The high-gain long-period (HGLP) seismograms were made available to us through Contract F44620–71–C–0082.

References

Arons, A. B. and D. R. Yennie (1950). Phase distortion of acoustic pulses obliquely reflected from a medium of higher sound velocity, *J. Acoust. Soc. Am.* **22,** 231–237.

Blatstein, I. M. (1971). Calculations of underwater explosion pulses at caustics, *J. Acoust. Soc. Am.* **49,** 1568–1579.

Burridge, R. (1963). The reflection of a pulse in a solid sphere, *Proc. Roy Soc. (London), Ser. A* **276,** 367–400.

Choy, G. and K. McCamy (1973). Enhancement of long-period signals by time-varying adaptive filters, *J. Geophys. Res.* **78,** 3505–3511.

Hill, D. P. (1974). Phase shift and pulse distortion in body waves due to internal caustics, *Bull. Seism. Soc. Am.* **64,** 1733–1742.

Jeffreys, H. J. and B. S. Jeffreys (1956). *Methods of Mathematical Physics*, 3rd ed., Cambridge University Press, 453–456.

Jeffreys, H. and E. R. Lapwood (1957). The reflection of a pulse within a sphere, *Proc. Roy. Soc. (London), Ser. A*, **241,** 455–479.

Richards, P. G. (1971). An elasticity theorem for heterogeneous media, with an example of body wave dispersion in the Earth, *Geophy. J.* **22,** 453–472.

Richards, P. G. (1973). Calculation of body waves for caustics and tunnelling in core phases, *Geophys. J.* **35,** 243–264.

Sachs, D. A. and S. Silbiger, (1971). Focusing and refraction of harmonic sound and transient pulses in stratified media, *J. Acoust. Soc. Am.* **49,** 824–840.

Savino, J. M., A. Murphy, J. M. W. Rynn, R. Tatham, L. R. Sykes, G. L. Choy, and K. McCamy (1972). Results of the high-gain long-period seismograph experiment, *Geophys. J.* **31**, 179–203.

Titchmarsh, E. C. (1926). Conjugate trigonometrical integrals, *Proc. Lond. Math Soc.* **2, 24,** 109–130.

Tolstoy, I., (1968). Phase changes and pulse deformation in acoustics, *J. Acoust. Soc. Am.* **44**, 675–683.

Lamont-Doherty Geological Observatory of Columbia University
Palisades, New York 10964
Contribution No. 2183

and

Department of Geological Sciences
Columbia University

Manuscript received June 24, 1974.